

Simulating Atmospheric Pollution Weathering on Buildings

N. Méryllou	S. Méryllou	D. Ghazanfarpour	J.M. Dischler	E. Galin
XLIM / DMI 83 rue d'isle 87000 Limoges, France nicolas.merillou@xlim.fr	XLIM / DMI 83 rue d'isle 87000 Limoges, France stephane.merillou@unilim.fr	XLIM / DMI 83 rue d'isle 87000 Limoges, France ghazanfarpour@unilim.fr	LSIIT, Pôle API, Bd Séb. Brant 67400 Illkirch, France dischler@dpt-info.u-strasbg.fr	LIRIS, 8, Bd Niels Bohr 69622 Villeurbanne eric.galin@univ-lyon2.fr

ABSTRACT

Interactions between polluted atmosphere and materials lead to an early aging of numerous buildings and monuments. This weathering process leads to important changes in appearance, from color blackening to small-scale geometric alterations: a black crust grows onto parts of affected surfaces, depending on the geometry of the object as well as on its environment. In this paper, we present a method to simulate this very important weathering process. Our method is physically inspired and provides full control to designers, keeping plausible results. First, specific polluted zones are detected according to their real physical classification. Then, the modifications of aspect of each zone are computed. Our results demonstrate that our model matches well the observed behavior of real-world monuments and buildings affected by atmospheric pollution.

Keywords : weathering, natural phenomena, shading, texture.

1. INTRODUCTION

Nearly all real world objects are submitted to aggressive environmental conditions. They react to these conditions by changes in appearances, which is usually called weathering. To achieve high realism in image synthesis, weathering of materials must be simulated as it contributes critically to the visual richness of images [Dorsey2008]. A vast variety of techniques have been proposed so far, following two main tendencies: models accounting accurately for specific weathering processes (for example [Dorsey96]), and more generic models usually based on texture transfer or synthesis techniques [Lu2007]). When the aging processes to be simulated strongly depend on the geometry of affected objects, specific techniques generally give very good results [Merillou2008].

Because of the increase, in our society, of energy production and consumption due to industry and transport development, the effects of pollution on buildings and cultural monuments are increasingly studied in numerous scientific fields. Damaging of monuments due to pollution is worrying from both economical and cultural heritage points of view. Indeed, a lot of money is spent in cleaning and restoring buildings and monuments.

Permission to make digital or hard copies of all or part of this work for personal or classroom use is granted without fee provided that copies are not made or distributed for profit or commercial advantage and that copies bear this notice and the full citation on the first page. To copy otherwise, or republish, to post on servers or to redistribute to lists, requires prior specific permission and/or a fee.

As outlined on figure 1, effects of polluted atmosphere on human constructions are visually very important. The goal of this paper is to propose a framework for visual simulation of atmospheric pollution. The problem of realistically reproducing the different weathering zones of a polluted object has not been specifically addressed so far in Computer Graphics. Our new algorithm main contributions are:

- a physically-inspired technique in order to provide plausible results;
- a local evaluation of the model providing a very good scalability to arbitrary scene complexity;
- an intuitive set of parameters to provide controllability for a designer.

Based on physics studies [Camuffo83], the effect of pollution onto surfaces is divided into two zones called by Camuffo et al. *black* and *white* zones. We propose to detect and render each without preprocessing step nor complex simulation. Moreover, our model is physically inspired: the way the surface is polluted is based on the physical processes described in [Lefevre2002].

The next section describes previous works concerning aging and weathering in computer graphics. Then in section 3, we review the numerous physical and chemical processes that lead to polluted surface appearance in order to provide a plausible model of the phenomenon. We describe the parameters that permit to control the effect. In section 4, we detail our method consisting in synthesizing on the fly specific textures linked to different polluted

zones. These textures are used to compute final aspect of the weathered object. We discuss obtained results in section 5. We finally conclude and present some possible future works.



Figure 1: Photos of a real polluted object (left) and the same object after cleaning (right).

2. RELATED WORK

In computer graphics, weathering phenomena are of great importance because of their major visual influence. Due to the large amount of different physical processes and their complexity, numerous studies have focused on specific phenomena. These techniques can be empirical or physically-based and can affect the entire rendering pipeline (geometry, reflectance properties, and colors). Becket and Badler [Becket90] have first handled surfaces imperfections by using a fractal based texture synthesis technique. Blinn [Blinn82] and Hsu [Hsu95] have proposed techniques to render surfaces covered by dust. Miller [Miller94] has provided accessibility shading algorithms permitting to render tarnished surfaces. Wong has proposed a geometry dependent method in [Wong97] to represent dust accumulation, patinas and peeling. In [Paquette01], authors modify objects geometry to handle impacts by different tools. Paint peeling and crackling have been investigated in [Paquette02]. In order to obtain more plausible results, some physically valid techniques have also been developed. Wet surfaces appearance has been studied in [Jensen99]. Corrosion (both patinas and destructive corrosion) has been investigated in [Dorsey96] and [Merillou2001]. A physically-based scratched surface model has been presented in [Bosch04]. A survey of weathering-related techniques has been presented in [Merillou2008].

Concerning building aging, specific studies have also been proposed. Dorsey [Dorsey96b] proposed a model to take into account dirtiness brought onto surfaces by flow processes. This technique permits to handle specific flow patterns on objects. Flows are only a small part of atmospheric pollution weathering. Weathering of stones has also been studied in [Dorsey99], including numerous

weathering processes handled by a model of their chemical reactions. Efflorescence, a porosity related aging phenomenon, has been studied in [Shahidi2005] using solid texture synthesis. Moreover, these two last studies handle weathering problems as physical simulations, but do not take into account the localization of the processes. This point has been addressed in [Chen2005]. Authors have introduced the γ -ton map, obtained by a pre-processing step: it is built from the abstraction of considering aging particles interacting with objects. Several weathering processes can be localized by this way, but have then to be specifically handled in term of rendering and the γ -ton map has to be rebuilt when geometry changes. In this paper, we focus our work on a physically inspired technique that does not need complete time-consuming simulations nor pre-processing step and still provides plausible results.

Several other techniques address the weathering problem. Replicating change in appearance by means of texture synthesis controlled by capture and transfer of weathering effects [Gu2006], [Lu2007] need acquisition devices that are not effective at the scale of real buildings. Atmospheric pollution weathering strongly depends on the object geometry itself, as well as on the surrounding geometry of other objects in the scene. Thus, texture transfer techniques seem inappropriate in our specific case.

3. ATMOSPHERIC POLLUTION

Among various kinds of building and monument degradations, atmospheric pollution is a major factor of change in appearance. Natural alteration processes are essentially due to weathering, i.e. thermal variation, humidity variation and bacteriological attack. However, all along the two previous centuries, the increase of energy production and consumption, due to transport and manufactures development as well as the use of new combustible (fuel, kind of fuels), has led to important sulphur emitting SO_2 under gaseous form and flying particles like soot. Thus, strong alteration of human constructions can be observed. Figure 2, presents a summary of the atmospheric pollution process consisting in three main steps.

Human activity produces numerous pollutants that fly into atmosphere such as SO_2 (that evolves to SO_3) and combustion particles. This is mainly observable in urban environments. These pollutants are transported into atmosphere and react with water (H_2O) to produce acid H_2SO_4 mixed with rain. This reaction is the first step of atmospheric pollution weathering as it creates acid rainfalls. In a second step, these acid rainfalls affect buildings and monuments and react with them. Building construction materials usually contain calcium

carbonates $CaCO_3$, that is able to react with water to create gypsum. This water mainly comes from rainfalls, but also from condensation due to fog for example [Delmonte97]. Gypsum that can be seen in our case as a grid that grows onto surfaces [Lefevre2002]. In the third and final step, dust and particles are trapped into the gypsum grid, creating a black crust that evolves from a few micrometers to a few centimeters.

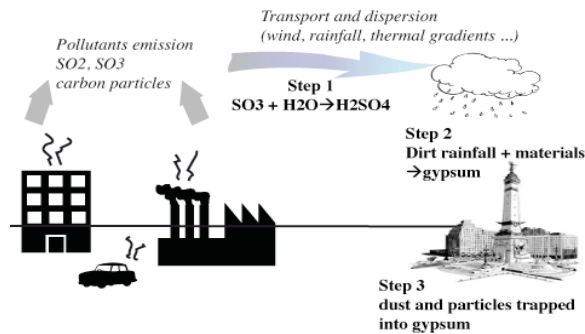


Figure 2: Summarizing the atmospheric pollution process into three main steps. Step 1: pollutants react with water to create (step 2) acid dirt rainfall that reacts with materials to create a gypsum grid. In step 3, particles are trapped into the gypsum grid.

It has been clearly established in physics [Camuffo83] that two behaviors have to be distinguished, due to different chemical reactions and inducing different appearances. This physical classification is based on two resulting appearances called *white* and *black* zones [Lefevre2002] (see figure 3).

White zones are directly submitted to strong rain impact and strong water streaming. These mechanical actions permit water to always clean up surfaces. Thus, in these areas, the material keeps its natural color. Each next rainfall evacuates particles deposited between two rainfalls, prohibiting gypsum grid creation.

Black zones: parts of objects that are not directly submitted to rainfalls or strong flows are not washed. However, the ambient moisture and weak flows permit the gypsum grid to develop itself without constraint. Blackening is due to the trapping of particles into the gypsum grid created on the objects external surface (see figure 2, step 3). The more the stone is porous, the more it traps moisture and the more the gypsum grid can develop itself.

4. MODELING AND RENDERING POLLUTED SURFACES

In order to propose a plausible modeling of atmospheric pollution of complete buildings, we need to perform two main steps. Firstly, differently

affected zones have to be detected with a local method in order to avoid complex transport simulations or complete surface flow modeling. Secondly, the reflectance properties of each zone have to be modified. Figure 4 presents the pipeline of our method.



Figure 3: Photo of a polluted object: white zones are washed by rainfalls or strong flows and remain protected from darkening, while the black zone is covered by pollution particles trapped into gypsum.

Zone detection

Recall from section 3 that *white* zones are found on surfaces directly exposed to rainfall or in zones washed by strong flows. Thus we have to simulate the different zones according to their interactions with rainfalls and to predict the possible flows onto the surface. Instead of a physical simulation of flows or transports [Dorsey96b], [Chen2005], we propose a physically inspired simple and intuitive model that does not need any precomputing phase. Thus we only need to compute direct rain accessibility, where droplets direct impacts can wash the surface. This rain accessibility rA has then to be combined with an estimation of strong flows rE , to fully characterize our zones.

4.1.1 Rain accessibility computation: rA

Our technique is a sort of directionally preferred ambient occlusion and is computed in a similar way as discussed in [Wong97]. Using ambient occlusion is a well-known trick in weathering simulation [Merillou08], and it can be easily adapted to simulate direct rain impacts by choosing plausible sampling directions. Over the time, rainfalls incident angles onto surfaces are guided by wind. Atmospheric pollution weathering is a long process: even if it starts as soon as a building or monument is exposed to pollutants, several years are often needed to observe important changes in appearance [Grieken98]. Thus, we propose to consider that rainfalls can come from every direction into a cone opened by angle α aligned with a direction vector V .



Figure 4: Summary of the method, from left to right: Porosity controlled by a noise texture – Computing rain accessibility rA – Computing strong flows and runs-out rfE – Computing reflectance modifications for final image.

Without any specific meteorological knowledge or artistic desire, we use classical values [Helming08] of rain incidence, leading in our model to $\alpha=20^\circ$ with V the vertical world axis. If the artistic desire is to orient rainfalls in a preferential direction, or if we have such knowledge in a specific geographic location, these parameters can be easily and intuitively modified. For example a preferential wind direction can be easily modeled by modifying V . We finally define a *directional occlusion* as the occlusion inside the previously described cone.

Moreover, washing intensity is also due to a combination of flow and material porosity [Camuffo95]: porous stones absorb water by capillarity, creating a black crust even in rain-exposed areas. We empirically propose to use directly the porosity values presented in table 1 in order to modulate rA . Porosity is described as a percentage of surface covered by pores, thus:

$$rA = (1 - porosity) * (1 - directional_occlusion)$$

The more the surface is porous, the more black crusts can develop. The porosity of building stones is described as a percentage of surface area covered by pores and evolves from 0% (for perfectly dense materials) to more than 50% (for very porous building materials). These values strongly depend on each material and are measured specifically in numerous studies, for example [Moropoulos09], [Sabbioni98], see table 1.

Material	Porosity
Carrara marble	0.6%
Verona red stone	8%
Portlandite mortars	18%
Limestone	0.5% to 23%
Clay bricks	27% to 47 %
Lime mortars	33% to 45%
Sandstone	1% to 30%

Table 1: Common and specific building materials porosity examples.

Moreover, this porosity value can exhibit strong variations, as shown on table 1, and even strong local

variations on a same surface, as measured by [Weishauptova2004]. We account for these variations with a Perlin noise [Perlin85].

4.1.2 Possible flow estimator: rfE

Strong water run-off on *black* zones can also lead to washing and thus to a shift into a white area [Camuffo95]. Thus, we propose to compute an estimator of strong flow: rfE . Here, we do not need to compute the full flow onto the surface, we only have to detect if the considered surface point is in a geometric configuration that favors a strong flow or not. These strong flows can come from :

- *border flows*: geometric features ending above the considered point can lead to strong flows (as observable below the corner of a window for example, see figure 5);
- *valley flows*: vertically-oriented geometric valley-like features (observable on a statue drape for example, see figure 6);

In order to propose a local estimator, we sample directions from the considered point in the local tangent plane situated at a distance d just above the surface. This distance permits the designer to define the size of the geometric features to consider, according to each 3D model.

Border flows estimator bfE . To detect *border flows*, we sample directions oriented along the vertical axis inside an angular region φ . In our implementation, we use raycasting at a distance maximum t_{max} . Each of the N intersection distance t_i is stored for all the sample rays. We do want to detect strong variations in values of t_i to detect obstacle that can potentially provide strong flows. Thus, we compute the standard deviation of the t_i values, normalized by the distance t_{max} . We also use a correction factor that accounts for the slope of the considered surface: the less the surface is vertical, the less border flows can be strong. Moreover, This leads to:

$$bfE = \frac{\sqrt{\frac{1}{N} \sum (t_i - t_{mean})^2}}{t_{max}} \sin(\angle(N, vertical))$$

Figure 5 shows the method and a result obtained on the front of a building. The parameters φ and t_{max} permit to control the desired shape of the run-outs.

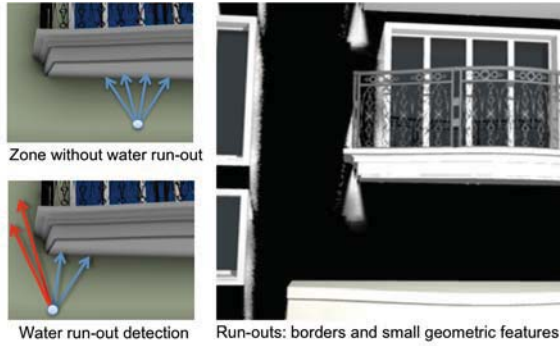


Figure 5: Border flows detection by sampling the geometry in the local tangent plane of the surface.

Valley flows estimator vfE . We use the same sampling than the previous one, but as we want to detect valleys, we create direction pairs by generating one sample direction inside a horizontal region (angle θ), and coupling it with its opposite direction in the local tangent plane (as illustrated on figure 6). Again with raycasting at a maximum distance t'_{max} we increase the number of hits h only when the two rays of a pair both intersect any geometry. The *valley occlusion* is defined as h/n_{rays} . Such sampling can also detect pits into the geometry, but as we are interested only in strong flows, we modulate vfE in the same way as bfE :

$$vfE = \frac{h}{n_{rays}} \sin(\angle(N, vertical))$$

Figure 6 presents examples of our valley-flows detection method on the *Athena* statue.

In order to keep a physically inspired model, we also have to account for the influence of porosity: the more the surface is porous, the less the flows are strong. Thus, we define the possible flow estimator rfE as:

$$rfE = (1 - porosity)(bfE + vfE)$$

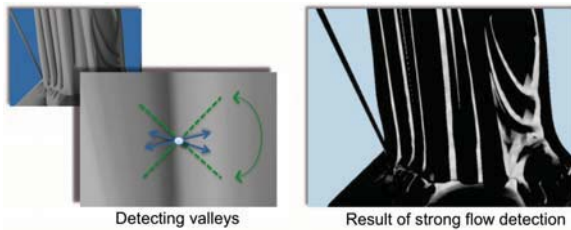


Figure 6: Valley flows local detection: pairs of sampling directions inside an horizontal region permit to localize valley-like geometric features.

Due to the phenomenology of atmospheric pollution weathering (see section 3), flows are only to be considered in *black* zones (previously detected by

rfE): *white* zones are already washed out. Note also that the main drawback of our proposed technique is that we cannot detect flows originating from other points of the object. The porous nature of building materials limits this problem (porous materials absorb water by capillarity) and permits to keep a local evaluation of pollution weathering. Finally, combining rfE and bfE at each renderer point gives us the local pollution rate P_R .

$$P_R = \begin{cases} 1 & \text{if } rfE + bfE > 1 \\ rfE + bfE & \text{otherwise} \end{cases}$$

Rendering: reflectance and surface alteration

As outlined in section 3, one of the consequences of atmospheric pollution is the soiling of building materials. In [Watt08] such visual nuisance can be measured as the reflectance contrast of a darkened area by comparison to the reflectance of the base surface. Thus, several models have been developed, based on experimental data, for predicting the rate of soiling. They postulates that the rate at which uncovered area becomes covered is proportional to the size of the uncovered area:

$$R = R_0 \left(\frac{A}{A_0} \right) + R_p \left(\frac{A - A_0}{A_0} \right)$$

With: R the object base reflectance, R_0 the reflectance from unaffected surface, R_p the reflectance from covering particles, A_0 the total area of surface that receives depositing particles and A the uncovered area of surface which receives depositing particles.

In atmospheric pollution weathering, the model for area coverage is usually an exponential function of exposure time [Pio98]:

$$A = A_0 \exp(-Kt)$$

With: K the soiling constant directly proportional to the polluted particles concentration C_p : $K = \lambda C_p$ (in physics, λ is the dose-response constant).

This leads to the evolution of reflectance as a function of exposure time:

$$R = (R_0 - R_p) \exp(-\lambda C_p t) + R_p$$

Since the concentration of pollutants strongly depends on various parameters such as the classification of the location (rural, urban, industrial...), we keep it as a user driven parameter that is directly related to the polluting rate. From our phenomenological point of view, we use the previously computed rate P_R as the evolution of polluted particles concentration: on washed parts, such concentration is minimum and on black areas, it is at its maximum. During the rendering step, this process progressively modulates the color of the darkened areas:

$$R = (R_0 - R_p) \exp(-P_R t) + R_p$$

R is then used as the base material reflectance in the designer chosen BRDF. Thus it can easily be ported to any real-time shading language (entry maps such as rain accessibility and flows can be pre-computed). Note that with black crust mainly composed of black carbon particles $R_p=0$.

As denoted in [Camuffo95], the black crust is dendritic, leading to a very rough irregular aspect. The thickness of this crust above affected surfaces is a few millimeters and depends on the porosity of the underlying material. Thus, to empirically account for this phenomenon, we simply add a rough bump mapping to the black crust rendering to account for such effect (we use a Fractional Brownian Motion perturbation). The depth of this bump map is modulated by the porosity of the material: the more the material is porous, the more the black crust is thick and dendritic.

5. RESULTS

The model presented in this paper has been implemented in our own realistic rendering engine. Note that as the pollution textures are computed *on the fly*, our method does not increase the renderer memory requirements. Figure 7 shows a clean and a polluted bunny with a thick bump mapped black crust. The top of the polluted bunny is submitted to rain fall and stays clean, while its bottom is polluted. Figure 8 shows the detection of flows on the geometric features of the column as well as detection of flows into corners. Figure 9 shows the progressive weathering of Athena due to atmospheric pollution. Different weathering rates are observable due to rain accessibility as well as strong flows. This example exhibits a strong porosity, reducing the *white* zone. Note that a homogeneous darkening of the surface cannot match the expected behavior.



Figure 7: Pollution with a design choice of a thick bumped black crust.

Figure 10 exhibits pollution evolution on a building and a zoom on specific patterns that shows the importance of zone detection in the atmospheric pollution weathering simulation. Rendering time of the clean building is 140s with our renderer and the polluted building is rendered in 200s (with 9 samples for rA and 9 samples for rfE).

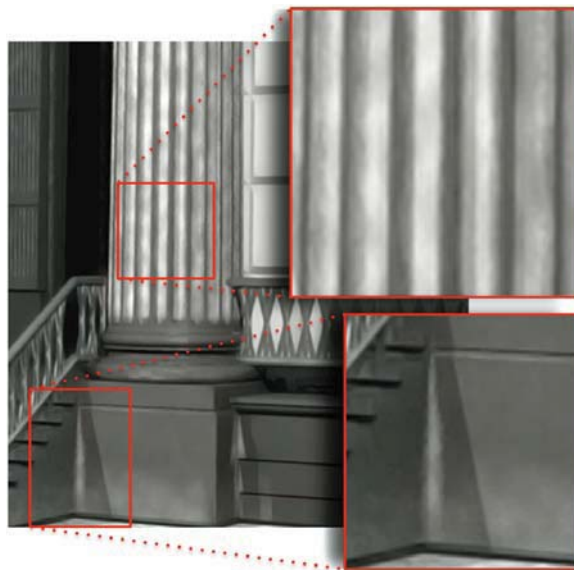


Figure 8: Importance of flow detection in the patterns observable on polluted objects.

Finally, figure 11 shows the ease of use and scalability of our model. As previously discussed, it relies on a local evaluation and does not need any iteration nor preprocessing step to choose the pollution level. The cost of our technique depends on the occlusion-like implementation. In our Monte-Carlo rendering engine, we rely on raycasting for such feature. Unpolluted building on figure 10 is computed in 49 seconds. The polluted building is computed in 75 seconds. This is due to the number of sample taken for zone detection (we use 16 samples for rA and 16 samples for rfE).

6. CONCLUSION AND FUTURE WORKS

In this paper, we have presented a method that permits to simulate, on a physically-inspired basis, the major effect of atmospheric pollution weathering. This specific weathering process is visually very important and contributes to improving realism of rendered images. Beyond this visual importance, this simulation can be useful in several other fields such as architecture or cultural heritage preservation as our tool permits to detect weathered zones (zones to protect with high priority). We are actually porting our method to GPU (OpenCL / CUDA) for interactive performance. Moreover, the physical analysis presented here makes our phenomenological approach simple and intuitive. As future works, we aim to improve our model in order to take into account other materials: metals and glasses are also affected by atmospheric pollution. We are also actively studying de-weathering possibilities as treatments to perform on real photos to virtually clean real objects.



Figure 9: Athena statue perfectly clean (left) and progressively affected by atmospheric pollution weathering.



Figure 10: A zoom on different patterns automatically detected on the front of a building (the left image is the clean building, for reference). Rain accessibility, porosity variations and strong flows are clearly observable.

7. AKNOWLEDGEMENTS

This work is supported by the French National Agency for Research (ANR) under agreement ANR-06-MDCA-004-01.



Figure 11: Our model is scalable and can render complex buildings and streets without complex physical simulation or preprocessing step.

8. BIBLIOGRAPHY

- [Becket90] BECKET, W., BADLER, N. I.: Imperfection for Realistic Image synthesis. *Journal of Visualization and Computer Animation*, 1, 1 (august 1990), 26-32
- [Blinn82] BLINN, J. F.: Light Reflection Functions for Simulation of Clouds and Dusty Surfaces. In *Computer Graphics (Proceedings of SIGGRAPH 82)*. (1982), vol. 16, pp. 21-29.
- [Bosch04] BOSCH, C., PUEYO, X., MERILLOU, S., GHAZANFARPOUR, D.: A Physically-Based Model for Rendering Realistic Scratches. *Computer Graphics Forum (Proceedings of Eurographics '04)*, 23, 3 2004), 361-370
- [Camuffo83] CAMUFFO, D., MONTE, M. D., SABBIONI, C.: Origin and Growth Mechanism of the Sulfated Crust on Urban Limestone. *Water, Air, and Soil Pollution*, 19, 1983), 351-359
- [Camuffo95] CAMUFFO, D.: Physical Weathering Of Stones. *The Science of Total Environment*, 167, 1995), 1-14

- [Chen2005] Chen Y, Xia L, Wong TT, Tong X, Bao H, Guo B, et al. Visual simulation of weathering by g-ton tracing. *ACM Transactions on Graphics* 2005;24(3):1127–33.
- [Delmonte97] MONTE, M. D., ROSSI, P.: Fog and Gyp- sum Crystals on Building Materials. *Atmospheric Environment*, 31, 11 1997), 1637-1646
- [Dorsey96] DORSEY, J., HANRAHAN, P.: Modeling and Rendering of Metallic Patinas. In *ACM SIGGRAPH*. (1996), pp. 387 - 396.
- [Dorsey96b] DORSEY, J., PEDERSEN, H. K., HANRAHAN, P.: Flow and Changes in Appearance. In *ACM SIGGRAPH*. (1996), pp. 411 - 420.
- [Dorsey99] DORSEY, J., EDELMAN, A., JENSEN, H. W., LEGAKIS, J., PEDERSEN, H. K.: Modeling and Rendering of Weathered Stone. In *ACM SIGGRAPH*. (1999), pp. 225 - 234.
- [Dorsey2008] DORSEY, J., RUSHMEIER, H., SILLION, F.: *Digital Modeling of Material Appearance*. Morgan Kaufmann/Elsevier. 2008.
- [Grieken98] GRIEKEN, R. V., DELALIEUX, F., GYSELS, K.: Cultural heritage and the environment *Pure and Applied Chemistry* 70 12 1998), 2327-2331
- [Gu2006] Gu J, Tu C, Ramamoorthi R, Belhumeur P, Matusik W, Nayar SK. Time-varying surface appearance: acquisition, modeling, and rendering. Boston: ACM SIGGRAPH; 2006.
- [Helming08] HELMING, K.: Wind Speed Effects On Rain Erosivity. *Geomorphology*, 94, 3-4 2008), 290-313
- [Hsu95] HSU, S., WONG, T.: *Simulating Dust Accumulation*. IEEE Computer Graphics and Applications, 15, 1 1995), 18-22
- [Jensen99] JENSEN, H. W., LEGAKIS, J., DORSEY, J.: Rendering of Wet Material. In *Rendering Techniques '99*. (1999), pp. 273-282.
- [Lefevre2002] LEFEVRE, R. A., AUSSET, P.: *Atmospheric Pollution and Building Materials: Stone and Glass*. Geological Society Special Publication : Natural Stones, Weathering Phenomena, Conservation Strategies and Case Studies, 205, 2002), 329-345
- [Lu2007] LU, J., GEORGHIADES, A. S., GLASER, A., WU, H., WEI, L. Y., GUO, B., DORSEY, J., RUSHMEIER, H.: Context-Aware Textures. *ACM Transactions on Graphics*, 6, 1 (January 2007)
- [Merillou2001] MERILLOU, S., DISCHLER, J. M., GHAZANFARPOUR, D.: Corrosion: simulating and rendering. In *Graphics interface 2001*. (2001).
- [Merillou2008] MERILLOU, S., GHAZANFARPOUR, D.: A survey of aging and weathering phenomena in computer graphics. *Comput. Graph.*, 32, 2 2008), 159-174
- [Miller94] MILLER, G.: Efficient algorithms for local and global accessibility shading. In *ACM SIGGRAPH*. (1994), pp. 319 - 326.
- [Moropoulos09] MOROPOULOS, A., POLIKRETI, K.: Principal Component Analysis in Monuments Conservation: Three Application examples. *Journal of Cultural Heritage*, 10, 2009), 73-81
- [Paquette01] PAQUETTE, E., POULIN, P., DRET-TAKIS, G.: Surface aging by impacts. In *Graphics interface 2001*. (2001).
- [Paquette02] PAQUETTE, E., POULIN, P., DRET-TAKIS, G.: The simulation of Paint Cracking and Peeling. In *Graphics Interface 2002*. (2002), pp. 59-68.
- [Pio98] A.PIO, C., RAMOS, M. M., DUARTE, A. C.: Atmospheric Aerosol and Soiling of External Surfaces in an Urban Environment. *Atmospheric Environment*, 32, 11 1998), 1979-1989
- [Perlin85] PERLIN K. An image synthesizer. In *SIGGRAPH '85 conference proceedings*, San Francisco, CA, July 22–26 1985, 1985, p. 287–96.
- [Sabbioni98] SABBIONI, C., ZAPPIA, G., GHEDINI, N., GOBBI, G., FAVONI, O.: Black Crust On Ancient Mortars. *Atmospheric Environment*, 32, 2 1998), 215–223
- [Shahidi2005] SHAHIDI, S., MERILLOU, S., GHAZANFARPOUR, D.: Phenomenological simulation of Efflorescence in brick constructions. In *Eurographics Workshop on Natural Phenomena*. (2005).
- [Watt08] WATT, J., JARRETTA, D., HAMILTONA, R.: Dose Response Functions for the Soiling of Heritage Materials due to Air Pollution Exposure. *Science of the Total Environment*, 400, 1-3 2008), 415-424
- [Weishauptova2004] WEISHAUPTOVA Z. PRIKRYL R. Porosimetric studies in rocks: methods and application for weathered building stones. *Dimension Stones 2004*, Taylor & Francis Group, London.
- [Wong97] WONG, T. T., NG, W. Y., HENG, P. A.: A Geometry Dependent Texture Generation Framework for Simulating Surface Imperfections. In *Proceedings of Eurographics Workshop on Rendering*. (1997), pp. 139 - 150